

## Micro-Scanning Laser Range Finders and Position-Attitude Determination for Formation Flight

Hirobumi Saito, Tatsuaki Hashimoto, Kenji Kasamura, and Hiroshi Goto\*

Institute of Space and Astronautical Science

3-1-1, Yoshinodai, Sagamihara, Kanagawa, Japan, 229

Phone/FAX: +81-42-759-8363, [koubun@newslan.isas.ac.jp](mailto:koubun@newslan.isas.ac.jp)

\* Omron Corporation, Japan

### Abstract

There are several space missions which require a cluster of micro spacecraft with small area of several kilometer. We propose an asteroid mission by means of several micro spacecraft in formation flight. We are in progress to develop a micro-scanning laser range finder (MS-LRF) for navigation system of such cluster missions. The MS-LRF is a LRF which utilized a two-dimensional scanner fabricated by micromachine technology. Also we propose navigation algorithm to determine the relative position and attitude of member spacecraft in the cluster using MS-LRFs.

### Introduction

There are many space missions where, instead of a large spacecraft, a cluster of spacecraft in formation flight executes the mission purpose. Examples of such cluster missions are the Global Positioning System (GPS), LEO/MEO constellations for communication system, and the global mapping of the geomagnetic sphere, all of which are global scale clusters.

On the other hand, a cluster of spacecraft scattered in smaller area (order of kilometers) may execute a new type of space missions. One example is the optical interferometry mission which is recently planned in the US. Another example is a cluster mission of asteroid observation such as imaging as well as measurements of the magnetic and the gravitational field.

Institute of Space and Astronautical Science (ISAS), Japan, will launch in 2002 the MUSES-C spacecraft, which is the asteroid sample return mission<sup>1</sup>. Figure 1 is an image of MUSES-C mission. The mission is to execute rendezvous with a near-earth asteroid 1989-ML, touch down, and collect pieces of the sample. Then the spacecraft will return to the earth and release a reentry capsule to be recovered in ground. In the early phase of MUSES-C mission planning, a new mission concept of micro spacecraft cluster was proposed<sup>2,3</sup>. This mission concept

will be described in a section of this paper, although this advanced mission concept was not selected.

The size of Asteroids is order of a kilometer, and the cluster of spacecraft has the size of several kilometers. Navigation of the spacecraft cluster in formation flight may require radio wave or optical measurements. Radio wave technique includes interferometric angle detection as well as ranging. The interferometric angle detection needs to have a certain length of baseline for interferometry in the spacecraft, which may be inadequate to a micro spacecraft.

Instead, optical technique may be promising in

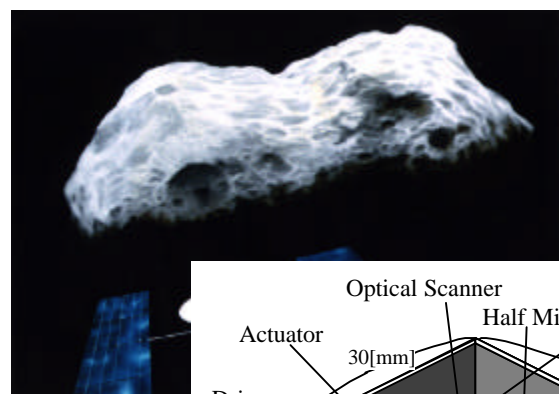


Fig. 1 Japan Mission "MUSES-C"

this range rather than

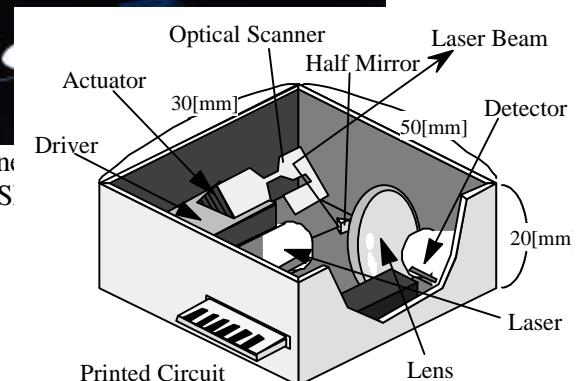


Fig.2 Concept of Micro-Scanning Laser Range Finder (MS-LRF).

the radio wave technique. Laser technique can measure both of range and angle. While an equipment for laser ranging is relatively easy to be applied to this purpose, scanning and tracking of the targets may be difficult for cluster missions. A conventional type of tracking laser radar can not track more than two targets, since the laser beam is usually narrow. Therefore, cluster missions require a scanning type of laser range finder, which is provided with capability to scan a laser beam in order to detect simultaneously many spacecraft in the cluster. Conventional scanning mechanisms in space, however, are very massive and consume large power since they utilize rotating mirrors driven by motors.

In this paper we propose a micro scanning laser range finder (MS-LRF), and the application to a cluster mission in smaller area (order of kilometers). A MS-LRF is a laser range finder with a 2-axis scanning mirror fabricated by means of micro-machining technology. MS-LRFs can detect other spacecraft in the cluster and measure the range and the direction. The proposed navigation algorithm makes it possible to determine not only the relative position but also the relative attitude of the daughter spacecraft. This paper describes the outline of MS-LRF under development and the new navigation algorithm by MS-LRFs to determine the relative position as well as the relative attitude.

### **Micro-Scanning Laser Range Finder**

#### ***Outline of MS-LRF***

Scanning laser range finders (LRF) have been applied in space missions. Conventional scanning mechanisms in space, however, are very massive and consume large power since they utilize rotating mirrors driven by motors.

Developments of microelectrical mechanical system (MEMS) have rapidly been achieved. Scanning mechanisms for laser beam are one of these achievements, since laser beam is massless and can be manipulated easily by micromachine. One of authors have been developing a micro two-dimensional optical scanner using a piezoelectric actuator<sup>4-7</sup>. The main applications of this scanner are supposed to be pattern recognition sensors at proximity range and imaging sensors for a small robot to inspect

inside pipes of nuclear power plants. As one of other applications, ISAS is in progress to apply this scanning mechanism to the laser range finder for cluster missions as well as for a planetary rover<sup>2,3</sup>. This micro-scanning mechanism will remarkably reduce the weight, size, and power consumption compared with the conventional sensors.

Figure 2 shows the conceptual model of the proposed micro-scanning laser range finder (MS-LRF), which consists of an optical scanner device, a micro lens, a beam splitter, a laser diode, an avalanche photo diode, a piezoelectric actuator to drive the scanner, drive circuits, and signal processing circuits. Table 1 summarizes the main characteristics of the MS-LRF. The optical configuration of MS-LRF is depicted in Fig. 3. Laser beam emitted from the laser diode is reflected at the beam splitter and is scanned at the micro-mirror. The collimated beam propagates through free space and is reflected back from the corner-cube reflector (CCR) on the other spacecraft in the cluster. The return

Mass	0.1kg
Size	5×3×2cm <sup>3</sup>
Power	3W
Laser Power	100mW
Laser Beam Divergence	0.22deg
Detection Range	Max 10kmfor 2cm CCR
Scanning Range	Max 90deg×60deg
Accuracy of Angle	0.3% of full range
Accuracy of Rangeng	1m
Scan Time	1s for one frame*

\*) condition is in the text.

Table 1 Predicted Performance of MS-LRF

beam propagates along the same optical path as the forward path to the beam splitter. Finally the return beam is detected by the sensitive avalanche photo diode.

MS-LRFs for cluster missions require high accuracy and high frame rate. The laser beam is amplitude-modulated cw wave. The intensity of the semiconductor laser is modulated simultaneously by two frequencies of 5kHz and 1MHz to measure range from 0.1km to 10km with accuracy of 1m.

#### ***Micro Two-Dimensional Scanner***

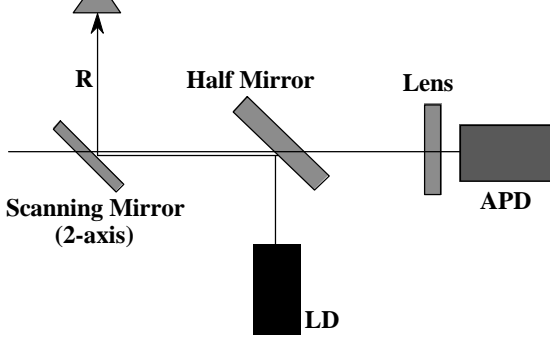


Fig.3 Optical Configuration of MS-LRF.

A miniature two dimensional scanner which

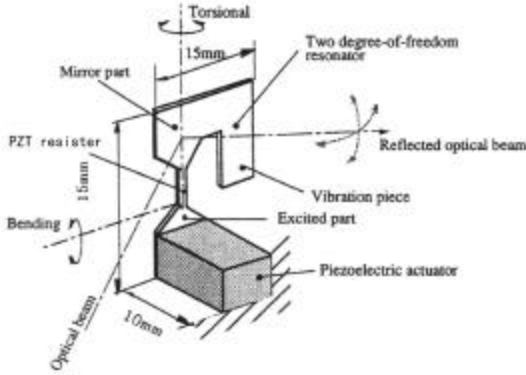


Fig.4 Structure of Micro Two-Dimensional Scanner.

has been developed <sup>4-7</sup> is shown in Fig.4. The scanner consists of two elements, a resonator and a piezoelectric actuator. Here the center of gravity is shifted from each rotational axis. The resonator has two eigen vibration modes, twisting and bending mode of the torsional spring as shown in Fig.4. Actuating the resonator with a piezoelectric device at each resonant frequency leads to the resonant vibration with a large amplitude. Each resonant frequency  $f_B$  and  $f_T$  (B:bending mode, T:twisting mode) is described by the following equation.

where  $K$  and  $I$  denote stiffness of torsional spring and rotational inertia moment  $c$  (1) resonator for the bending mode and the twisting mode, respectively. Typical values of resonant frequency  $f_B$  and  $f_T$  are 100 - 400 Hz. When a voltage of  $f_B$  frequency and one of  $f_T$  frequency are superimposed to the piezoelectric actuator, both modes are simultaneously excited with large amplitudes. Figure 5 is an example of full scanning angle  $2\theta_B$  and angle  $2\theta_T$  of laser beam as functions of applied voltage to the piezoelectric actuator. Full scanning angles of bending direction and twisting direction in atmosphere condition are 80 degree and 50 degree, respectively. In vaccum these angles extend to more than 90 degree and 60 degree,

SSC99-VI-1

respectively, since air drag plays important role in the motion of scanner<sup>7</sup>.

As a result, optical beam reflected on the mirror of the vibrating resonator can be scanned in the two-dimensional of bending angle  $\theta_B$  and twisting angle  $\theta_T$ . The scanning pattern results in Lissajous figure as shown in Fig. 6. When  $f_B$  and  $f_T$  are not in rational ratio, the beam scans continuously in the area of  $2\theta_B \times 2\theta_T$ , taking

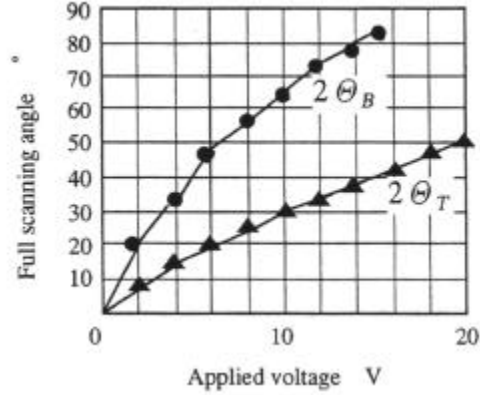


Fig.5 Full Angle of Beam Scanning by Micro-Scanner.

finite size of the beam into account. Scanning time of the beam in the full scanning angles depends on the scanning angles, the laser beam divergence, the resonant frequencies  $f_B$  and  $f_T$ . As an example, it takes about 1 second to scan the area of 50deg×20 deg by means of MS-LRF of  $f_B = 70.74\text{Hz}$  and  $f_T = 348.7\text{Hz}$ , beam divergence 0.22 deg. The scanning time increases to 10 second for a narrow beam of divergence 0.11deg.

The scanning angle is detected by a piezoresistor which is fabricated at position of the torsion spring as shown in Fig.4. Resistance of the piezoresistor, which depends on the stress at the torsion spring, is measured by a external circuit. Signal of the measured resistance is applied to two sets of narrow band pass filters with center frequency  $f_B$  and  $f_T$ . Outputs from the two filters are proportional to the bending and twisting angle position,  $\theta_B$  and  $\theta_T$ . This angle detection technique is found to have accuracy of  $\pm 0.3\%$  of full scanning angle for temperature variation of  $\pm 10$  degree<sup>7</sup>.

Link Analysis

$$r_r = p \cdot \frac{r_h}{r_c} (1 - r_h) r_m^2 r_c T$$

$$\left[ \begin{matrix} D \\ \vdots \end{matrix} \right]^2 \left[ S \cdot \cos 45^\circ \right]$$

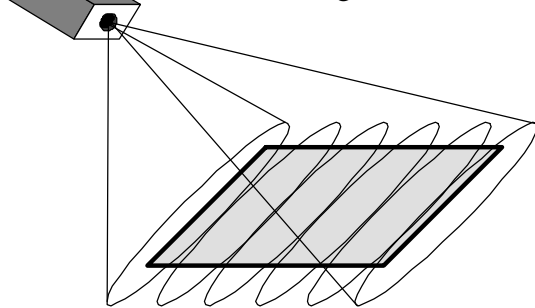


Fig.6 Scanning Pattern of MS-LRF.

This section describes link analysis for detection of micro spacecraft with corner cube reflectors by means of micro-scanning laser range finders (MS-LRFs)<sup>3</sup>. Optical configuration (2) is shown in Fig.2. Receiving signal  $I_r$ [A] laser beam is given by where

- $P_0$ : power of laser diode = 100 mW
- $\eta_t$ : efficiency of transmitter optics = 0.7
- $\eta_h$ : reflectance of half mirror = 0.5
- $\eta_m$ : reflectance of scanning mirror = 0.9
- $\eta_c$ : reflectance of CCR = 0.9
- $T_L$ : efficiency of receiver optics = 0.9
- $D_c$ : effective diameter of CCR = 2 cm
- $R$ : range between spacecraft
- $\theta$ : divergence angle of laser beam = 4 mrad
- $D_L$ : diameter of collimeter lens = 2 mm
- $S$ : area of scanning mirror = 4 cm<sup>2</sup>
- $R_0$ : sensitivity of APD = 0.5 A/W

$$I_{sn} = \sqrt{2qI_rFB}$$

$$I_{am} = N_{ep} \sqrt{BR_0M}$$

$M$ : amplification gain of APD = 100.

Noise currents in the receiver are the shot noise  $I_{sn}$  and the amplifier noise  $I_{am}$ . They are given as where

- $q$ : charge of electron (3)
- $F$ : noise coefficient = 3.98
- $B$ : bandwidth of amplifier = 1 MHz
- $N_{ep}$ : noise equivalent power =  $3.0 \times 10^{-14}$  W/ Hz.

Link analysis is performed for various

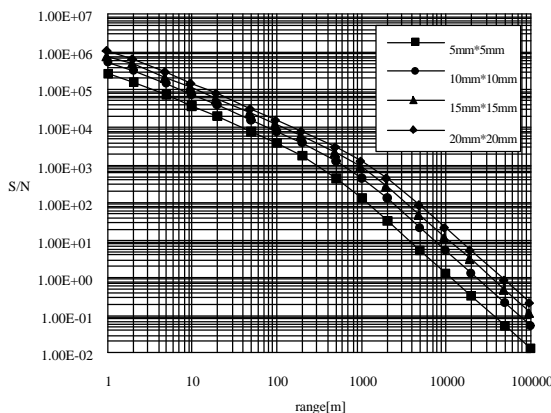


Fig.7 Signal-to-Noise Ratio of MS-LRF for CCR Target

## SSC99-VI-1

parameters of the system. Figure 7 is an example of signal-to-noise ratio S/N, where plots are shown for four sizes of CCR. When a corner cube reflector with 2cm in diameter, signal-to-noise ratio S/N is 20 for 10 km range. This range is typical size of the micro spacecraft in formation flight of our interest.

### Cluster Mission of Asteroid as Example

In this section, a new mission concept of asteroids by means of a cluster of micro spacecraft is proposed. The micro-scanning laser range finders are utilized to determine relative position and attitude of the micro spacecraft. The navigation algorithm by means of MS-LRFs, which is proposed here, can be applied to other kinds of cluster missions.

Size of asteroids is from several 10 meters to several 10 kilometers. The target of MUSES-C mission is 1989-ML. Size of 1989-ML is expected to be 0.5-2 km in diameter. Sphere of influence for the asteroid is about 10 km. Mapping of the image, the gravity field and the magnetic field in this range are important science missions. It, however, is risky for a single spacecraft to fly to the shadow region of the asteroid or to approach to the surface. Exploration by a single spacecraft may not be the best scenario. The best scenario may be a mission by a mother spacecraft and a cluster of many micro spacecraft, in order to execute intensive survey.

Size	12×12×10cm <sup>3</sup>
Mass	2.0kg
MS-LRF×2	0.2kg
CCR×6	0.2kg
Magnetometer	0.2kg
Transmitter	0.2kg
Antenna	0.1kg
Processor	0.3kg
Battery	0.3kg
Solar Cell	0.2kg
Strut/Cable	0.3kg

Table 2 Concept of Daughter Spacecraft

The image of the cluster mission of an asteroid in formation flight is shown in Fig.8. Mother spacecraft is provided with all functions of interplanetary cruise from the earth to the asteroid. A cluster of micro spacecraft (daughter spacecraft) is released from the mother spacecraft. The number of the micro spacecraft

is more than two, and a large number is better for the mission. The micro spacecraft should be as simple as possible to reduce the mass. The total weight of daughter spacecraft is about 2 kg. Table 2 shows the outline of the daughter spacecraft. Each daughter spacecraft is provided only with a MS-LRF, passive corner-cube reflectors (CCR), a radio transmitter to the mother spacecraft, primary battery (or solar cells and secondary battery), and some mission sensors such as a magnetometer and a camera. The daughter spacecraft does not have inertial sensors and radio receivers. The mother spacecraft is equipped with inertial attitude sensors to measure the inertial attitude of itself, the receiver for the daughter spacecraft, MS-LRFs and the corner cube reflectors.

Each daughter spacecraft executes the science mission at the position. MS-LRF in the daughter spacecraft keeps scanning to detect other spacecraft in the cluster. Then the MS-LRF of each daughter spacecraft measures range and direction from itself to the other spacecraft in the body-fixed coordinate system. Each daughter spacecraft sends telemetry data to the mother spacecraft.

The mother spacecraft receives the data from all the daughter spacecraft. Then the mother spacecraft can determine the relative position and the relative attitude of all the daughter spacecraft. The algorithm of the determination is described in the next sections. This navigation processing is required for the scientific data from daughter spacecraft. The magnetic fields which

are measured in the body-fixed coordinate of the daughter spacecraft are converted to the field components in the inertial coordinate. The orbital data of daughter spacecraft around the asteroid is

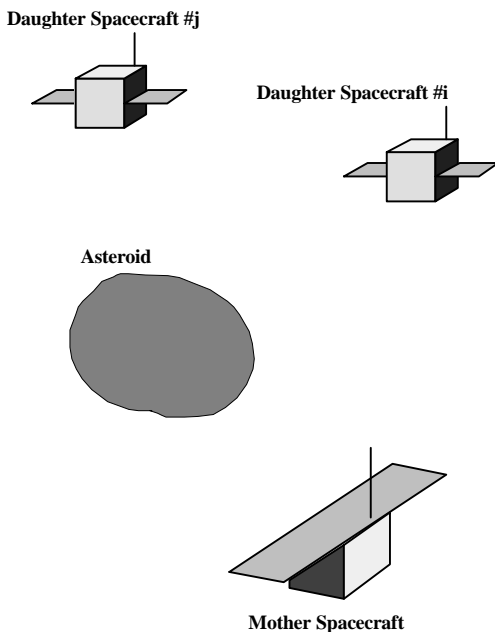


Fig.8 Image of Asteroid Mission by Micro Spacecraft Cluster in Formation Flight

utilized to determine the gravity field and the mass distribution of the asteroid. The camera data requires both of the attitude and the position.

**Determination of Position and Attitude**

The MS-LRFs can measure and estimate relative positions, relative attitudes of the spacecraft, or both of them, depending on the mission purpose. There are several cases of the navigation scenarios. Figure 9 shows three cases. Case (1) is that the mother spacecraft #0 determines the relative positions of other spacecraft #i and #j in the cluster. Since the MS-LRF in the mother spacecraft #0 can detect the relative vectors of other spacecraft, the measurement and estimation are simply executed in the mother spacecraft #0.

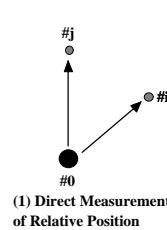


Fig.9 Three MS-LRFs.

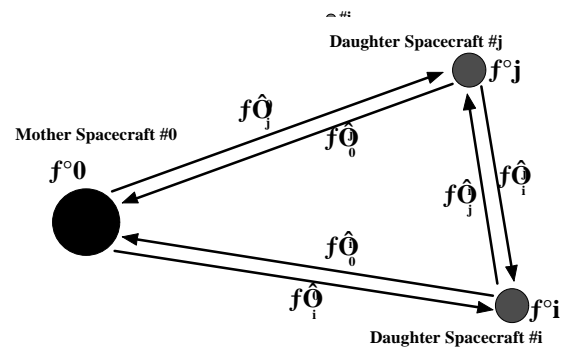


Fig.10 Attitude Determination by MS-LRFs.

Case (2) is that the mother spacecraft detects the relative attitude of the daughter spacecraft #i by means of MS-LRF in the mother spacecraft #0 and telemetry data from the daughter spacecraft #i. The daughter spacecraft #i measures the relative positions of #0 and #j, and transmits the data of MS-LRF to the mother spacecraft #0. This navigation algorithm is described in the next section.

Case (3) is the GPS-like position determination. When positions of the three spacecraft #0,#i,#j are known, position of spacecraft #k can be determined by only range data. Since most of 3-dimensional range sensors like MS-LRF have better accuracy in range measurements but worse in angle measurements, the GPS-like position determination is expected to improve

$$\begin{bmatrix} y_j^i \\ z_j^i \end{bmatrix} = \begin{bmatrix} R_j^i \cos \mathbf{d}_j^i \sin \mathbf{a}_j^i \\ R_j^i \sin \mathbf{d}_j^i \end{bmatrix}$$

## SSC99-VI-1

the component perpendicular to line-of-sight direction. This navigation system will be presented in different chances by the authors.

### Formalism of Navigation

#### *Member of Cluster*

A cluster of spacecraft consists of one mother spacecraft (spacecraft #0) and N daughter spacecraft (spacecraft #1, #2, #N). The body-fixed coordinate of spacecraft #j is denoted by  $\mathbf{r}_j^i$ . All the spacecraft have MS-LRFs and corner-cube reflectors on the surfaces. Furthermore, the daughter spacecraft is provided with a radio transmitter, some mission sensors, and primary battery (or solar cell and secondary battery). The mother spacecraft is provided with attitude sensors and a radio receiver. All the navigation calculation is executed only in the mother spacecraft. It is assumed that all spacecraft are always visible each other.

Each spacecraft searches other spacecraft in the cluster by means of MS-LRF. As Fig.10 shows, the spacecraft #i detects the spacecraft #j (j ≠ i) and measures the direction and range  $(\mathbf{d}_j^i, R_j^i)$  of the spacecraft #j in the body-fixed coordinate  $\mathbf{r}_i^i(x_i, y_i, z_i)$  of the spacecraft #i. In practice a MS-LRF controls the scanning mirror with the bending angle  $\alpha_T$  around the x-axis and the twisting angle  $\alpha_B$  around the y-axis as is shown in Fig.4. For sake of simplicity of this analysis, the direction is expressed in terms of the azimuthal angle  $\mathbf{d}_j^i$  and the elevation angle  $\mathbf{a}_j^i$ . The position vector  $\mathbf{x}_j^i = (x_j^i, y_j^i, z_j^i)$  of the spacecraft #j is expressed in the body-fixed coordinate  $\mathbf{r}_i^i(x_i, y_i, z_i)$  as

(5)

Although the daughter spacecraft #i and #j are shown in Fig.10, N daughter spacecraft are assumed. As a whole of the cluster, total number of the measurements is N(N+1) of observation vectors.

#### *MS-LRF data on Mother Spacecraft*

The MS-LRF in the mother spacecraft measures the position vectors of all the daughter spacecraft as

$$(\mathbf{r}_j^0, \mathbf{d}_j^0, R_j^0), \text{ for } j=1,2, \dots, N \quad (6)$$

The mother spacecraft, however, can not identify the true identification number #j of the daughter spacecraft by means of MS-LRF data alone. The identification of daughter spacecraft will be discussed later.

#### *Telemetry Data from Daughter Spacecraft*

All the daughter spacecraft transmit their own telemetry data to the mother spacecraft. The data format is as followed:

$$\{ \#i, (\mathbf{r}_0^i, \mathbf{d}_0^i, R_0^i), (\mathbf{r}_j^i, \mathbf{d}_j^i, R_j^i), \text{Data } i \} \text{ for } i=1, \dots, N, \text{ and } j \neq i \quad (7)$$

where the true identification number #i of the daughter spacecraft is transmitted to the mother spacecraft. The "Data i" in the telemetry includes the science mission data obtained in the spacecraft #i such as magnetic field measurements and image data of the asteroid. Since there are N daughter spacecraft in the cluster, interferences between communication links have to be avoided. There are several concepts to solve the similar problem in radio wave communications and mobile communications. Time division multiple access (TDMA) is hardly applicable, since our system is one-way communication and signal of synchronization can not be transmitted to the daughter spacecraft. Candidates are frequency division multiple access (FDMA) and code division multiple access (CDMA). The latter may be promising since technology developments of the CDMA are very rapid in mobile communications and GPS receivers.

#### *Identification of Daughter Spacecraft*

The mother spacecraft can not identify the true identification number of the daughter spacecraft which is detected as  $R_j^0$  in (6) by MS-LRF of the mother spacecraft. The mother spacecraft finds the most probable spacecraft number #I among the telemetry data of the range  $R_j^0$  in (7) from the daughter spacecraft such that  $R_j^0 = R_I^0$ . The range errors of MS-LRFs are about 1 m, and the size of the cluster is from 1km to 10 km. Therefore, error probability of identification is considered to be very low. Alternative algorithm to identify the the number of the daughter spacecraft is to apply technique of pattern matching to the position vector data (5), and (6). Such technique is also used for star identification

of a star tracker sensor.

Finally, the mother spacecraft acquires  $N(N+1)$  vector data of the relative position observation from the mother spacecraft itself as well as from  $N$  daughter spacecraft as expressed by

$$\left( \begin{matrix} \mathbf{x}_j^i \\ \mathbf{R}_j^i \end{matrix} \right) \quad \text{for all } i, j=1,2, \dots, N, i \neq j \quad (8)$$

### Estimation of Relative Attitude

In this section, we propose least-squares estimation algorithm for relative attitudes of  $N$  daughter spacecraft in a cluster. The relative attitude of a daughter spacecraft # $i$  is expressed by the rotation matrix  $C_i$ , which transfers a vector in the body-fixed coordinate  $\mathcal{O}_0$  of the mother spacecraft to a corresponding vector in the body-fixed coordinate  $\mathcal{O}_i$  of the daughter spacecraft. As Fig.9 explains, the observation vector  $-\mathbf{x}_i^0$  in  $\mathcal{O}_0$  system is transformed to the  $\mathbf{x}_i^i$  vector in  $\mathcal{O}_i$  system by the rotation matrix  $C_i$ .

$$\mathbf{x}_i^i = C_i (-\mathbf{x}_i^0). \quad (9)$$

Similarly, the relative position vector  $\mathbf{x}_j^i - \mathbf{x}_i^i$  from the daughter spacecraft # $i$  to # $j$ , which is based on measurements in the mother spacecraft system  $\mathcal{O}_0$ , is transformed to the observation vector  $\mathbf{x}_j^i$  in the # $i$  daughter spacecraft system  $\mathcal{O}_i$ .

$$\mathbf{x}_j^i = C_i (\mathbf{x}_j^0 - \mathbf{x}_i^0) \quad \text{for all } i, \text{ and } j, j \neq i. \quad (10)$$

As a matrix form

$$\begin{pmatrix} \mathbf{x}_1^i \\ \mathbf{x}_2^i \\ \dots \\ \mathbf{x}_N^i \end{pmatrix} = C_i \begin{pmatrix} -\mathbf{x}_i^0 \\ \mathbf{x}_1^0 - \mathbf{x}_i^0 \\ \mathbf{x}_2^0 - \mathbf{x}_i^0 \\ \dots \\ \mathbf{x}_N^0 - \mathbf{x}_i^0 \end{pmatrix} \quad \text{for daughter spacecraft #}i, \text{ and } j \neq i. \quad (11)$$

Determination of relative attitudes of daughter spacecraft in the cluster results in a mathematical algorithm to obtain most probable estimation of the rotation matrix  $C_i$  based upon two sets of  $N$  observed vectors. The left-hand side of (11) is based on the vectors observed in the daughter spacecraft # $i$ , and the right-hand side of (11) is based on the vectors observed in the mother spacecraft.

### Least-Squares Estimation of Relative Attitude

The most clear algorithm to estimate the rotation matrix  $C_i$  in terms of mathematics seems the least-squares estimation (LSE) algorithm. Reference [8] analyzed the similar problem in relation with vision pattern matching. According to ref.[8], the least-squares estimation of the

rotation matrix  $C_i$  is given as follows. First, the matrices  $Y$  and  $X$  are defined as

$$Y = (\mathbf{x}_0^i, \dots, \mathbf{x}_j^i, \dots, \mathbf{x}_N^i), \quad (12)$$

$$X = \begin{pmatrix} -\mathbf{x}_i^0 \\ \mathbf{x}_1^0 - \mathbf{x}_i^0 \\ \mathbf{x}_2^0 - \mathbf{x}_i^0 \\ \dots \\ \mathbf{x}_N^0 - \mathbf{x}_i^0 \end{pmatrix} \quad (13)$$

which appeared in both sides of (10). The matrix  $Y X^T$  is a  $3 \times 3$  observation matrix of this system. When number of observation vector

$$S = \begin{cases} I, \det(YX^T) \geq 0 \\ \text{diag}(1,1,-1), \det(YX^T) < 0 \end{cases}$$

$\mathbf{x}_j^i$  is not less than 3, rank of  $Y X^T$  is 3. Let a singular value decomposition of  $Y X^T$  be  $U D V^T$ , where  $D$  is a  $3 \times 3$  diagonal matrix  $\text{diag}(d_1, d_2, d_3)$ ,  $d_1 \geq d_2 \geq d_3 > 0$ , and  $U, V$  are  $3 \times 3$  orthogonal matrices. Then the least-squares estimation of the rotation matrix  $C_i$  is given by

$$C_i = U S V^T \quad (14)$$

where

### Numerical Simulation for Relative Attitude (15)

Monte Carlo simulations of relative attitude estimation are performed, based on the least-squares estimation described in the previous section. Many simulations are performed for various parameters of measurement errors of MS-LRF and configuration of spacecraft in a cluster. Several examples of the results are shown here. Figure 11 is the configuration of five spacecraft (#0, #1, #2, #3, #4) in a cluster. The maximum size of the cluster is 2.8 km. The coordinate system in Fig.10 is the body-fixed

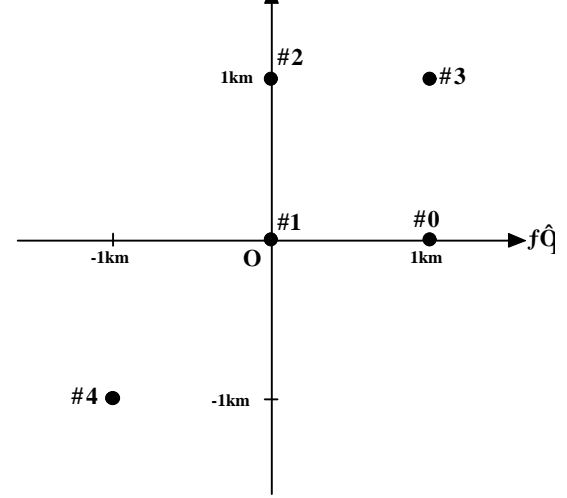


Fig.11 Configuration of Spacecraft Cluster in Formation Flight for Monte Carlo

Error of Sensor			Estimation Error of #1 S/C Attitude		
R (m)	(deg)	(deg)	(deg) <sup>x</sup>	(deg) <sup>y</sup>	(deg) <sup>z</sup>
1.0	0.0	0.0	0.0	0.0	0.0
0.0	0.2	0.0	0.0	0.0	0.21
0.0	0.0	0.2	0.4	0.29	0.01
0.0	0.2	0.2	0.42	0.28	0.21
1.0	0.2	0.0	0.0	0.0	0.20
1.0	0.2	0.2	0.39	0.27	0.21

Table 3 LSE of Relative Attitude for Three Spacecraft

coordinate system  $\Sigma_1$  of the daughter spacecraft #1 for sake of simplicity. Errors of measurements are assumed to be random. Based on expected accuracy of MS-LRF described in the previous chapter, standard deviations are selected to be 1 meter for range, and 0.2 deg for azimuth and elevation measurement.

Results of Monte Carlo simulations with 1000 trials are shown in Table 3 and 4, assuming various combinations of measurement errors. In Table 3, the cluster consists of three spacecraft #0, #1, and #2. The attitude of the daughter spacecraft #1 is measured and estimated in the mother spacecraft #0 by means of the LSE algorithm. The estimation errors of the attitude are described in terms of small Euler angles  $\alpha_x, \alpha_y, \alpha_z$  in the body-fixed coordinate  $\Sigma_1$ . It is found that the errors of the attitude is almost independent from the range errors  $R$ . The angle errors (azimuth angle error) and (elevation angle error) of MS-LRFs are dominant in this parameter region, where the angle error is  $\alpha = 0.2 \text{ deg} = 3.5 \times 10^{-3} \text{ rad}$  and the relative range error is  $R/R = 1 \text{ m}/1\text{km} = 1 \times 10^{-3}$ . Essentially, the range data is utilized only when the relative position vector  $\mathbf{x}_j^o - \mathbf{x}_i^o$  between #i and #j daughter spacecraft are calculated. The errors of the relative attitude are as large as the angle error of MS-LRF such as  $\alpha = (1 \sim 2) \times (\alpha \text{ or } \beta)$ .

In Table 4, the attitude of the daughter spacecraft #1 is estimated in the mother spacecraft for various cluster configurations. As the number of the spacecraft in the cluster increases, the estimation errors decrease. This is because errors of each MS-LRF may be

Spacecraft Configuration	Estimation Error of #1 S/C Attitude		
	$\alpha_x$ (deg)	$\alpha_y$ (deg)	$\alpha_z$ (deg)
3 S/C(#0,#1,#2)	0.39	0.27	0.20
4 S/C(#0,#1,#2,#3)	0.30	0.25	0.20
4 S/C(#0,#1,#2,#4)	0.29	0.25	0.20
5 S/C(#0,#1,#2,#3,#4)	0.26	0.23	0.16

Table 4 LSE of Relative Attitude for Different Spacecraft Configuration

averaged effectively as number of measurements by MS-LRFs increases.

The two cases of 4 spacecraft in Table 4 indicate that the estimation error does not sensitively depend on a geometrical configuration of the spacecraft in the cluster. This may be because in this navigation system the attitude is estimated based mainly on the angle measurements of MS-LRF. The error of ranging is almost negligible. On the other hand, performance of navigation system such as Global Navigation System, which is based on range measurements alone, depends sensitively on the geometrical configuration. Concept of dilution-of-position (DOP) describes this characteristic.

**Conclusion**

We propose an asteroid mission by means of several micro spacecraft in formation flight. We are in progress to develop a micro-scanning laser range finder (MS-LRF) for navigation system of such cluster missions. The MS-LRF is a LRF which utilized a two-dimensional scanner fabricated by micromachine technology. Also we propose navigation algorithm to determine the relative position and attitude of member spacecraft in the cluster using MS-LRFs.

The relative attitude can be estimated at the mother spacecraft by means of the MS-LRF in the mother spacecraft and the telemetry data of the MS-LRF in the daughter spacecraft. This algorithm is based on the least-squares-estimation of pattern matching between the MS-LRF data taken in the mother spacecraft and the daughter spacecraft. It is found that angle errors of MS-LRFs are dominant over range errors. Estimation errors of attitude are as much as angle accuracy of MS-LRFs, and are almost independent from geometrical configuration of the cluster.

**References**

1. Kawaguchi,J., Uesugi,K., et al, "Sample and Return Mission in 2002 to Nereus via Electric Propulsion", IAF-95-Q.5.05, 1995.
2. Nakatani,I.,Saito,H.,Kubota,T., Mizuno,T., Kato,T., Nakamura,S., Kasamura,K., and Goto,H., "Mirco Scanning Laser Range Sensor for Planetary Exploration," Int. Conf. Integrated Micro/Nanotechnology for Space Application, Houston, USA, Oct, 1995.

3. Kasamura,K., "Study on Micro Laser Range Sensor with Two Dimensional Scanning Mechanism for Space Application," Master Thesis of Univ. of Tokyo, March, 1997.
4. Goto,H., and Imanaka,K., "Super Compact Dual Axis Optical Scanning Unit Applying a Torsional Spring Resonator Driven by a Piezoelectric Actuator," Proc. of SPIE, Vol.1544, pp.272-281,1991.
5. Goto,H., "Two-Dimensional Micro Optical Scanner Excited by PZT Thin Film Microactuator," Proc. of SPIE, Vol.3419,pp.227-235, 1998.
6. Ikeda,M., Totani,H., Akiba,A.,Goto,H., Matsumoto,M., and Yada,T., "PZT Thin-film Actuator Driven Micro Optical Scanning Sensor by 3D Integration of Optical and Mechanical Devices," 12th IEEE Int. Conf. MEMS,pp.435-440, Orlando, USA, Jan, 1999.
7. Goto, H., "Study on Compact Two-Dimensional Scanning Mechanism and Application to Imaging Sensor in Small Robot," Doctor Thesis of Tokyo Institute of Technology, Jan.,1999.
8. Umeyama, S., "Least-Squares Estimation of Transformation Parameters Between Two Point Patterns," IEEE Trans.Pattern Analysis and Machine Intelligence, vol.13,no.4, pp.376-380, 1991.